

Fast Low Angle Positive Contrast Steady-State Free Precession (FLAPS) Imaging : Theory and Experiment

R. Dharmakumar¹, I. Koktzoglou², and D. Li^{1,2}

¹Radiology, Northwestern University, Chicago, IL, United States, ²Biomedical Engineering, Northwestern University, Chicago, IL, United States

Introduction It is well known that magnetic susceptibility variations lead to signal voids in MRI. However, recent work [1-3] has shown that positive contrast imaging of susceptibility-induced field variations can provide signal enhancements rather than signal losses. Here we propose a new method, Fast Low Angle Positive contrast SSFP (FLAPS), for rapidly acquiring off-resonance positive contrast images. Our hypothesis is that by taking advantage of the spectral response of the steady-state free precession (SSFP), it may be possible to generate signal enhancement from off-resonant spins while suppressing the signal from on-resonant spins at relatively low flip angles (Fig. 1). The fundamental idea of FLAPS-based off-resonance contrast is captured in Fig. 1.

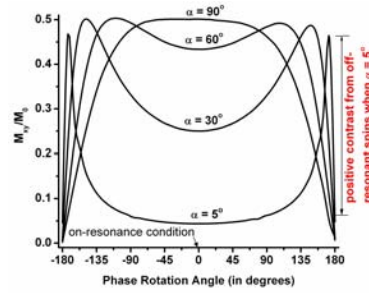


Fig. 1. Figure shows the expected dependence of SSFP signal intensity (M_{xy}/M_0) on phase rotation angle (due to off resonance frequency shifts) and the excitation flip angle (α). Note that the signal difference between the on- and off-resonant spins is strongly dependent on α .

Theory Starting from SSFP signal equations [4], it is possible to show that in the presence of a magnetic perturber in a medium, a positive signal difference between off- and on-resonant spins (in the presence of phase cycling), at a spatial location \mathbf{r} from the magnetic perturber, can be written as

$$C(\beta(\mathbf{r})) = M_0 \sin \alpha \left[\frac{\sqrt{2(1 + \cos \beta(\mathbf{r}))}}{2(T_1/T_2)(1 - \cos \alpha) + \cos \beta(\mathbf{r})(1 + \cos \alpha) + \cos \alpha + 1} - \frac{1}{(T_1/T_2)(1 - \cos \alpha) + \cos \alpha + 1} \right], \quad \text{if } 0 < \alpha < \arccos\left(\frac{T_1/T_2 - 1}{T_1/T_2 + 1}\right)$$

where M_0 is the equilibrium magnetization; T_1 and T_2 are spin-spin and spin-lattice relaxation constants; α is the flip angle; $\beta(\mathbf{r}) = \Delta\omega T_R$, where $\Delta\omega$ is the frequency shift induced by the magnetic perturber at \mathbf{r} and T_R is the repetition period. From here, one can show that the spatial extent of the positive contrast is strongly dependent on T_1/T_2 , α , and $\Delta\omega$. It was found that, for a given T_1/T_2 of the imaging medium, there is an optimum α which generates the greatest positive contrast and it decreases with increasing T_1/T_2 .

Methods In order to validate the theoretical findings, phantom and *ex-vivo* tissue studies were performed using a cylindrical tube containing 50 μM Fe (Feridex I.V., Advanced Magnetics, USA). All experiments were performed on a whole-body 1.5T scanner (Siemens, Germany) using a head coil for signal reception. Imaging parameters common to phantom and tissue studies: coronal imaging slices, field-of-view = $20 \times 20 \text{ cm}^2$, matrix = 512×512 , slice thickness = 5 mm, $T_R = 6.5 \text{ ms}$, acquisition time for each scan = 3.3 s, and α between $5^\circ - 90^\circ$ (5° increments). The T_1 and T_2 of the phantom and each tissue were measured using inversion-recovery and multiple spin-echo experiments, respectively. **Phantom Experiments:** The cylinder containing ferumoxide solution was immersed in a saline bath and imaged. **Tissue Experiments:** To evaluate the dependence of optimum α generating the greatest positive contrast on T_1/T_2 , experiments were performed using *ex-vivo* lamb blood, liver, and heart tissues. The cylindrical perturber was inserted into each tissue type, and the tissues (except blood) were immersed in saline and imaged. **Data Analysis:** Contrast-to-noise ratio (CNR), defined as $\text{CNR} = (S_{PC} - S_B)/\sigma_N$ where S_{PC} , S_B , and σ_N , denote the positive contrast signal, background signals, and standard deviation of noise were computed for both phantom and *ex-vivo* tissue studies.

Results & Discussion **Phantom Experiments:** T_1/T_2 value at 1.5T for the water bath was 1.3. It was observed that there is an optimum α ($\sim 35^\circ$) which generates the greatest positive contrast (Figs. 2 and 3). **Tissue Experiments:** T_1/T_2 values at 1.5T for *ex-vivo* blood, liver, and heart were 5.0, 7.2, and 12.5, respectively. It was observed that the optimum α determining the greatest positive contrast was dependent on tissue type (T_1/T_2) and is indirectly related to T_1/T_2 . Optimal α in blood, liver, and heart at 1.5T were approximately 25° , 20° , and 10° , respectively. Optimum CNR values obtained in the various tissues are collected in Fig. 4. Based on theory and experiments, we have demonstrated that the SSFP method can be sensitized to generate positive contrast signals from off-resonant spins with the appropriate choice of α . Experiments validated the theoretical predications that positive contrast is strongly dependent on α and T_1/T_2 . Future work needs to address the impact of $\Delta\omega$ and T_R on FLAPS-based positive contrast.

Conclusion This study demonstrated that the FLAPS technique is ideally suited for rapid imaging with off-resonance positive-contrast using low flip angles. These advantages may be utilized for real-time tracking of passive interventional devices and/or time-efficient 3D positive contrast imaging of labeled cells.

References [1]Cunningham CH, MRM 2005;53:999; [2] Stuber M, 13th ISMRM p. 2608; [3] Mani V, MRM 2006;55:126; [4] Mansfield P, 1982 *NMR in Biomedicine*.

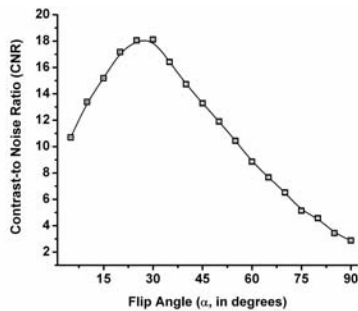


Fig. 2: Experimentally observed dependence of FLAPS-based CNR on flip angle (α) for the cylindrical tube containing ferumoxide solution placed in a saline bath. As α increases CNR increases, peaks around 35° , and then decreases to nearly zero as α approaches 90° .

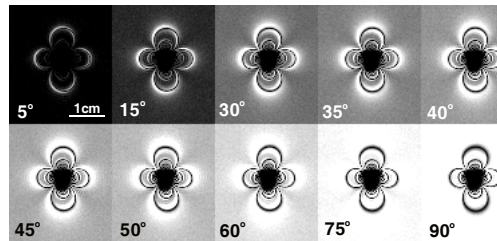


Fig. 3: Experimentally obtained images showing positive contrast from a cylinder containing ferumoxides placed in a saline bath. Note that the spatial extent of the positive contrast increases with α , peaks around 35° , and then decreases to nearly zero at higher α .

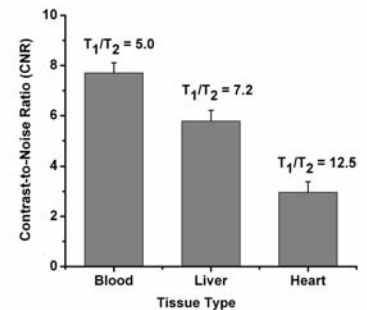


Fig. 4: Experimentally observed peak CNR values from the *ex-vivo* tissue studies at the optimal α . Note that, consistent with the theoretical prediction, CNR decreases as T_1/T_2 increases.